

# Alignment, Electronic Properties, Doping, and On-Chip Growth of Colloidal PbSe Nanowires

Dmitri V. Talapin,<sup>\*,†,‡,§</sup> Charles T. Black,<sup>‡</sup> Cherie R. Kagan,<sup>‡</sup> Elena V. Shevchenko,<sup>†,‡</sup> Ali Afzali,<sup>‡</sup> and Christopher B. Murray<sup>‡</sup>

The Molecular Foundry, Lawrence Berkeley National Laboratory, Berkeley 94720, California, and IBM Research Division, T. J. Watson Research Center, 1101 Kitchawan Road, Yorktown Heights, New York 10598

Received: May 29, 2007; In Final Form: June 26, 2007

Single-crystalline straight, zigzag, helical, and branched nanowires can be synthesized by oriented attachment of PbSe nanocrystals followed by their fusion in the presence of different surfactants. These colloidal nanowires can be aligned in external electrical fields, facilitating their integration into electronic circuits. We show how the nanowire morphology affects the interaction of nanowires with the electric field. Conducting PbSe nanowires can be assembled from nanocrystal building blocks directly on a chip, growing along the electric field. As-formed PbSe nanowires show a *p*-type conduction that can be switched to an *n*-type by charge-transfer doping of the nanowires with hydrazine. In this work, we demonstrate strategies for device integration of solution-phase synthesized semiconductor nanowires and explore their electronic properties.

## Introduction

Semiconductor nanowires are promising materials for many nanotechnology-related applications, such as high-performance nanoscale field-effect devices,<sup>1</sup> logic gates,<sup>2</sup> memories,<sup>3</sup> sensors for gases and biomolecules,<sup>4</sup> thermoelectric devices,<sup>5</sup> LEDs and lasers,<sup>6,7</sup> photodetectors, and solar cells.<sup>8,9</sup> All these applications require high-quality semiconductor nanowires. Nanowires with good structural and electronic characteristics can be synthesized via seeded vapor–liquid–solid (VLS) growth using CVD or pulsed laser deposition techniques.<sup>10,11</sup> However, some important applications (e.g., solar cells, displays, printable electronic circuits, or thermoelectric devices) require large quantities of nanowires at a reasonably low price. Solution-phase synthetic methods, such as solution–liquid–solid growth<sup>12</sup> or oriented attachment,<sup>13,14</sup> are now extensively explored to provide desirable low-cost routes to the preparation of single-crystalline semiconductor nanowires.

Recently, we have demonstrated that chaining PbSe nanoparticles followed by their fusion through the oriented attachment is a method for fabricating high-quality PbSe nanowires with tailorable straight, zigzag, helical, or branched morphologies.<sup>15</sup> This technique is naturally suitable for the large scale production of colloidal nanowires. Owing to excellent semiconducting and thermoelectric properties of bulk lead chalcogenides (direct band gap, small effective masses for electrons and holes, high carrier mobilities, very large static dielectric constants, high thermoelectric figures of merit, etc.), colloidal PbSe nanowires may find use in transistors, thermoelectric coolers and heat converters, solar cells with carrier multiplication, infrared photodetectors, etc.<sup>16</sup>

Reliable, high-throughput techniques for positioning and alignment of semiconductor nanowires are very important for their integration into electronic and optoelectronic devices. To date, several experimental approaches have been explored: flow-

assisted alignment in a microfluidic channel,<sup>17</sup> Langmuir–Blodgett technique,<sup>18</sup> and electric field-directed alignment.<sup>19,20</sup> The last approach seems to be the most promising because it allows for the rapid assembly of complex (i.e., multidirectional) networks for nanowire-based electronic circuitry and readily lends itself to very short length scales.<sup>21</sup> In this work, we studied device integration strategies for solution-phase synthesized semiconductor nanowires and explored electronic properties of PbSe nanowires synthesized by the oriented attachment mechanism.

## Experimental Procedures

**Nanowire Synthesis.** The synthesis of PbSe nanowires with different morphologies has been described in detail in ref 15. Briefly, PbSe nanowires are synthesized by reacting lead oleate with trioctylphosphine selenide in a phenyl ether solution in the presence of oleic acid. Dipole–dipole interactions between PbSe nanocrystals orient them into chains as shown in Figure 1a,b. At high reaction temperatures (250 °C), the individual PbSe nanocrystals are fused and annealed into single-crystalline nanowires. The addition of co-surfactants (alkylphosphonic acids, alkylamines, etc.) is used to tailor the growth kinetics of different nanocrystal facets<sup>22</sup> and to control the morphology of PbSe nanowires. As examples, the addition of *n*-tetradecylphosphonic acid results in the straight nanowires shown in Figure 1c and Figure S1 in the Supporting Information. Dodecyl- or hexadecylamine co-surfactants allowed us to obtain zigzag and helical nanowires shown in Figure 1d–g. Branched PbSe nanowires (Figure 1h) are synthesized using primary amines as co-surfactants and precisely controlling the temperature profile during the reaction.<sup>15</sup> As-synthesized PbSe nanowires can be isolated from the reaction mixture by centrifugation and redispersed in chloroform, forming stable colloidal solutions.

**Alignment of PbSe Nanowires Using Electric Field.** Applying a dc electric field ( $10^4$  to  $10^5$  V cm<sup>-1</sup>) to a colloidal solution of PbSe nanowires allowed us to align the nanowires along the field. In a typical experiment, PbSe nanowires (~1 mg) were dispersed in 1 mL of an octane/nonane (1:1

\* Corresponding author. E-mail: dvtalapin@uchicago.edu.

† LBNL.

‡ T. J. Watson Research Center.

§ Current address: Chemistry Department, The University of Chicago, Chicago, IL 60637.

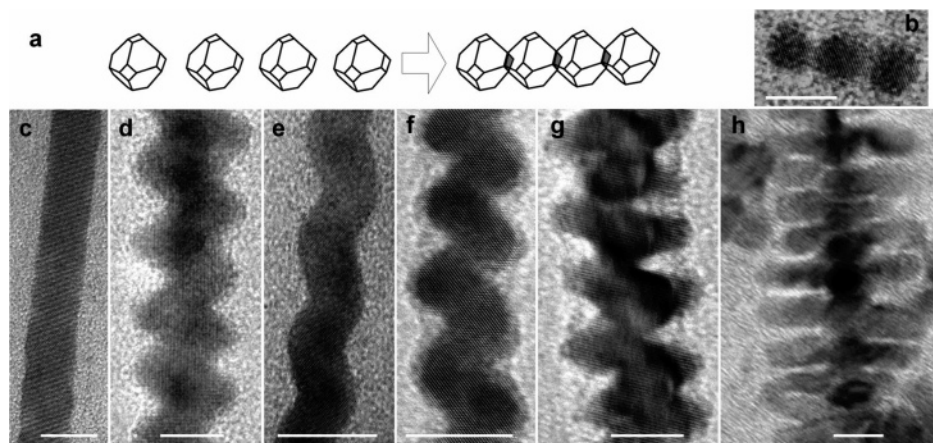


**Figure 1.** PbSe nanowires synthesized by oriented attachment of PbSe nanocrystals. (a) Schematic representation of the oriented attachment process. (b) High-resolution TEM image of a trimer formed at the early stage of reaction. TEM images of PbSe nanowires with (c) straight, (d) zigzag, (e–g) helical, and (h) branched morphologies. Scale bars, 10 nm.

vol/vol) mixture, and 10  $\mu\text{L}$  of a 10 wt % solution of hexadecene-graft-polyvinylpyrrolidone copolymer ( $M_n = \sim 7300$ , Aldrich, further referred to as HD-PVP) in nonane was added to improve the solubility of the PbSe nanowires. Gentle sonication of this solution for  $\sim 10$  s allowed us to prepare stable dispersions of PbSe nanowires in alkanes.

A silicon chip with a 150 nm thick layer of a thermally grown  $\text{SiO}_2$  layer and patterned parallel Ti/Au (75  $\text{\AA}$ /350  $\text{\AA}$ ) electrodes was used as a substrate. To make the  $\text{SiO}_2$  surface more hydrophobic, we treated the chips with hexamethylenedisilazane (HMDS) for 30 min at 150  $^\circ\text{C}$ . The electric bias (2–50 V) was applied between the gold electrodes spaced 0.2–40  $\mu\text{m}$  apart, generating a dc electric field of adjustable strength. A microdroplet (0.4–1  $\mu\text{L}$ ) of the nanowire solution has been precisely positioned to cover the gap between the electrodes, and the solvent was allowed to evaporate. After solvent evaporation, aligned PbSe nanowires were pinned to the surface by van der Waals forces, and the chip was carefully rinsed first with ethanol and then with hexane to wash out any impurities (e.g., residual HDE-PVP) left behind after solvent evaporation. The sample device was then dried in a vacuum and investigated using high-resolution SEM.

**On-Chip Growth of PbSe Nanowires.** The 7 nm diameter PbSe nanocrystals were thoroughly washed from an excess of capping ligands by several precipitation–dissolution steps (ethanol–toluene) and were redispersed in toluene. The toluene solution was left in the dark for about 1 week. At this stage, the capping ligand depleted PbSe nanocrystals slowly assembled into 60–100 nm long nanorods via the mechanism of oriented attachment.<sup>15</sup> The nanorod solution was strongly diluted with a chloroform/octane (1:1 v/v) mixture. Applying a dc electric field ( $1 \times 10^5$  to  $2 \times 10^5$   $\text{V cm}^{-1}$ ) to this solution resulted in spontaneous assembly of nanorods into semiconducting nanowires, which grew between biased electrodes. After complete solvent evaporation, the samples were studied by HRSEM.

**Electrical Measurements.** Nanowire-based devices were tested using an Agilent 4156B semiconductor parameter analyzer. The source electrode was grounded, and a highly doped Si wafer served as the back gate electrode. All room-temperature electrical measurements were performed under a dry nitrogen atmosphere to prevent oxidation and to improve reproducibility.

**Doping PbSe Nanowires with Hydrazine.** As-synthesized PbSe nanowires showed a *p*-type gate effect, suggesting that holes are the major carriers in the as-synthesized PbSe nanowires capped with oleic acid. The treatment of nanowire devices

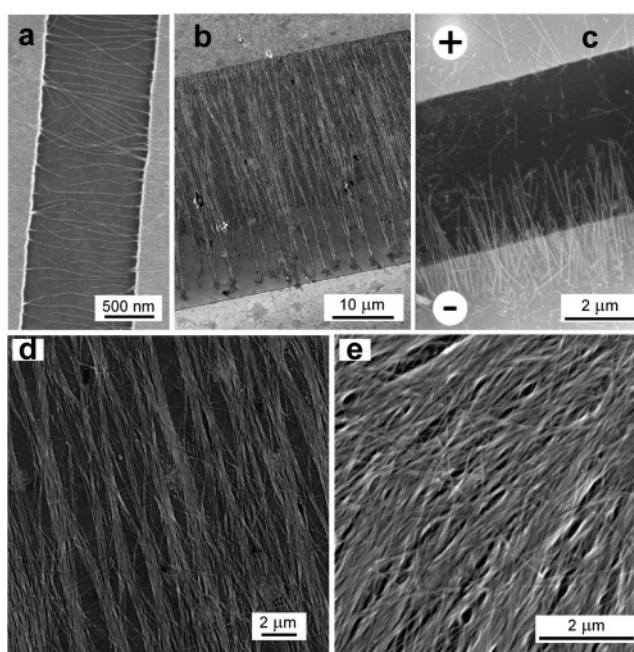


**Figure 2.** Alignment of straight sub-10 nm diameter PbSe nanowires by a dc electric field. Nanowires aligned across (a) 2  $\mu\text{m}$  and (b) 40  $\mu\text{m}$  channels. (c) Alignment process starts at the negatively biased electrode; short nanowires can be selectively pulled toward the negative electrode. (d and e) Arrays of aligned PbSe nanowires.

with a 1 M solution of hydrazine in acetonitrile for 0.5–1 min switched the gate effect from the *p*- to the *n*-type and increased the nanowire conductance by  $\sim 3$  orders of magnitude. The hydrazine solution could be applied to the entire chip or locally delivered using a microcapillary.

## Results and Discussion

**Alignment of PbSe Nanowires in dc Electric Fields.** The dc electric field can align colloidal PbSe nanowires in solution, generating various nanowire patterns. The evaporating carrier solvent allows for easy transfer of aligned nanowires on a substrate (Figure 2) and can be utilized for the fabrication of nanowire-based devices. Typically, 0.4–1  $\mu\text{L}$  of nanowire solution was deposited and left to evaporate between two Au electrodes patterned on a  $\text{SiO}_2$  surface. The nanowire packing density depended on the concentration and volume of the nanowire solution and could be varied over a broad range, from well-separated individual nanowires (Figure 2a) to thick films

of unidirectional nanowires (Figure 2d,e). Unidirectional alignment of PbSe nanowires was observed across electrodes with spacing ranging from 0.2 to 40  $\mu\text{m}$  (cf. Figure 2a,b) and applied electric field strengths from  $10^3$  to  $10^5$   $\text{V cm}^{-1}$ . We found that the mechanical properties of sub-10 nm diameter PbSe nanowires differed substantially from the properties of the respective bulk material. Unlike bulk PbSe, which is brittle, the nanowires easily bend (Figure S1 in Supporting Information) to follow the solvent flow patterns and directions of the electric field.

Both the electric field strength and the solvent evaporation rate have to be optimized to achieve unidirectional alignment of PbSe nanowires. For example, individual nanowires can be aligned and deposited from chloroform solutions, but the high evaporation rate is not conducive to obtaining densely packed and well-aligned nanowire assemblies. Adding  $\sim 5\%$  of the higher boiling point solvent tetrachloroethylene (TCE) to the chloroform solution allowed for more uniform nanowire alignment. The best results have been achieved using a mixture of alkanes (octane/nonane,  $\sim 1:1$  by volume). PbSe nanowires do not form a stable solution in alkanes, slowly bundling together and precipitating on the time scale of about a week. The nanowire solubility can be substantially improved by adding a small amount of HD-PVP. PVP chains have an affinity for the PbSe nanowire surface, while the grafted hexadecene groups provide sterical stabilization of the PbSe nanowires in nonpolar alkanes.

The interaction of a nanowire with an electric field depends on its charge, dipole moment, and polarizability. All these parameters are important in controlling and directing nanowire assembly using electric fields.<sup>21,23</sup> For example, if nanowires possess both longitudinal dipole moments and a net electrical charge, they can be both aligned and pulled toward one electrode. We found that the charging state of the PbSe nanowires can be adjusted by adding surfactant molecules to the nanowire solution. Thus, after adding a small amount of oleic acid to the solution containing only short (2–3  $\mu\text{m}$ ) PbSe nanowires, all nanowires can be aligned and selectively pulled toward the negatively biased electrode (Figure 2c). This is in agreement with our earlier finding that in the presence of oleic acid, PbSe nanocrystals hold a small positive charge (typically  $+e$  or  $+2e$  per nanocrystal).<sup>24</sup> Introducing a charge through surface derivitization can be used to control nanowire alignment and positioning by external electric fields.

A dc electric field applied to a solution of branched PbSe nanowires results in a distinctively different type of nanowire assembly. Instead of a uniform film of unidirectional nanowires, we observed nearly equidistant “nanoropes” formed by nanowire bundles as shown in Figures 3a,b. We hypothesize that side branches generate local transverse dipoles that interact with each other, causing the nanowires to assemble into uniform bundles. Another interesting emerging behavior has been observed for relatively short ( $\sim 1$   $\mu\text{m}$ ) PbSe “nanocentipedes”.<sup>15</sup> Their head and tail morphology is formed by side branches whose length gradually varies along the wire (inset in Figure 3c,d). In weak electric fields ( $< 10^4$   $\text{V/cm}$ ), the side-by-side and head-to-head pairing of individual nanocentipedes is predominant (Figure 3c). The side-by-side pairing can be energetically favorable if it provides efficient coupling of permanent longitudinal dipoles. Additionally, head-to-head pairing (Figure 3c) suggests a strongly nonuniform distribution of positive and negative charges along the length of the nanocentipede and demonstrates the important role of side branches in electrostatic interactions. The nanocentipede pairs orient along the electric field due to

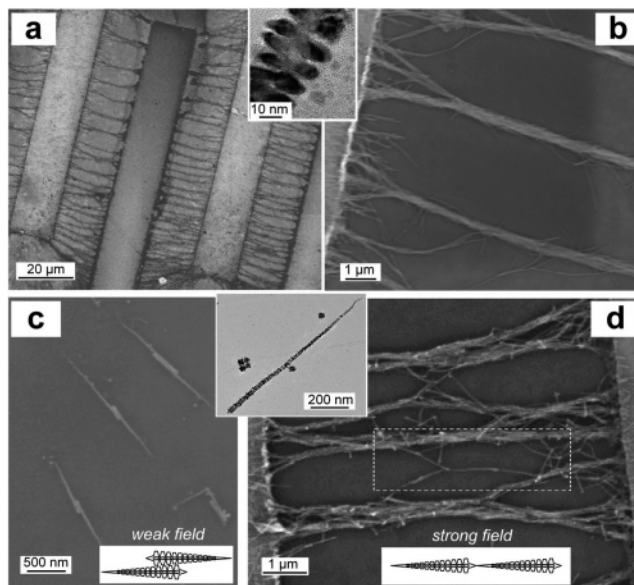


**Figure 3.** Alignment of branched PbSe nanowires by a dc electric field. (a and b) Branched PbSe nanowires assemble into nanoropes, which bridge the gap between biased electrodes. Inset shows a TEM image of a PbSe nanowire with a branched morphology. PbSe nanocentipedes demonstrate head-to-head and side-by-side coupling in a weak  $< 10^4$   $\text{V/cm}$  electric field (c), while head-to-tail coupling is dominant in strong  $\sim 10^5$   $\text{V/cm}$  electric field (d). Inset shows a TEM image of a PbSe nanocentipede.

their polarization by an external field. In strong electric fields ( $\sim 10^5$   $\text{V/cm}$ ), we observed the formation of nanoropes with a dominant head-to-tail assembly of the nanocentipedes (Figure 3d). In the case of head-to-tail coupled “centipedes”, the interaction between longitudinal dipoles and the external electric field provides an additional energy of  $-2\mu E$ , where  $\mu$  is the dipole moment, and  $E$  is the electric field strength. In a strong field, this term can dominate, switching the coupling from side-by-side to head-to-tail.

**Charge Transport in PbSe Nanowires and Nanowire Assemblies.** Three terminal measurements of PbSe nanowire FETs (Figure 4a) show that the current through the PbSe nanowires deposited on top of the Au source and drain electrodes can be modulated by applying a potential to the back gate electrode (Si wafer). Field-effect devices with as-synthesized PbSe nanowires show a *p*-type gate effect and low-field resistances of  $\sim 0.2$ – $1$   $\text{G}\Omega$  per the  $\sim 8$  nm diameter 2  $\mu\text{m}$  long nanowire (Figure 4b). The current modulation is on the order of  $I_{\text{on}}/I_{\text{off}} = \sim 10^3$  (Figure 4c). The current through PbSe nanowires can also be modulated by illuminating the nanowire devices as shown in the inset to Figure 4b.

The low conductance of the as-synthesized PbSe nanowire devices puts limitations on their electronic applications. However, we found that the nanowire conductance can be increased by about 3 orders of magnitude through charge-transfer doping with hydrazine. Short-term ( $\sim 30$  s) exposure of the nanowire device to a 1 M  $\text{N}_2\text{H}_4$  solution in acetonitrile converts the *p*-type nanowire FET into *n*-type FET with a current modulation of  $> 10^5$  and resistance in the on state of  $\sim 2$   $\text{M}\Omega$  per the  $\sim 8$  nm diameter 2  $\mu\text{m}$  long nanowire (Figure 4d,e). This approach works equally well both for short channel length devices (200 nm) with a single nanowire (Figure 4f) and for large arrays of PbSe nanowires aligned across long (tens of micrometers) gaps between source and drain electrodes (Figure 4g). These results demonstrate the applicability of charge-transfer doping for ultra-small circuits and large area electronic and optoelectronic

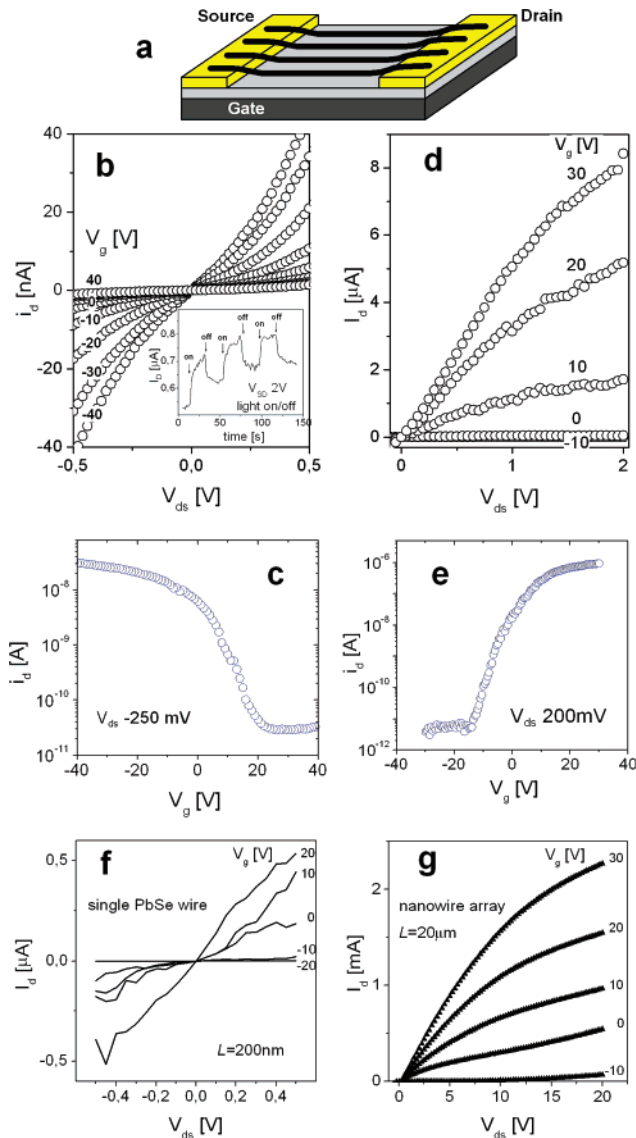


**Figure 4.** Transport properties of aligned straight PbSe nanowires. (a) Schematics of our nanowire field-effect devices. (b–e) Measurements performed on the same field-effect device with 18  $\sim 8$  nm diameter PbSe nanowires bridging a  $2 \mu\text{m}$  gap between source and drain electrodes. (b) Plot of drain current  $I_d$  vs drain-source voltage  $V_{ds}$ , as a function of gate voltage  $V_g$  for as-synthesized  $p$ -type PbSe nanowires. Inset shows the modulation of drain current by illuminating PbSe nanowires with visible light. (c) Plot of  $I_d$  vs  $V_g$  measured at constant  $V_{ds}$  of  $-250$  mV for as-synthesized  $p$ -type PbSe nanowires. (d and e) Plots of  $I_d$  vs  $V_{ds}$  at different  $V_g$  values and  $I_d$  vs  $V_g$  at  $V_{ds}$  of  $200$  mV, respectively, measured on the same device after  $n$ -type doping of nanowires by hydrazine. (f) Plot of  $I_d$  vs  $V_{ds}$  at different  $V_g$  values for a single  $8$  nm diameter PbSe nanowire  $n$ -FET with  $200$  nm channel length. (g) Plot of  $I_d$  vs  $V_{ds}$  at different  $V_g$  values for a dense array of  $n$ -PbSe nanowires aligned across a  $20 \mu\text{m}$  channel between source and drain electrodes.

devices. We found that single  $8$  nm PbSe nanowires can transmit currents up to about  $1 \mu\text{A}$ , corresponding to current density of  $2 \times 10^6$  A  $\text{cm}^{-2}$ . The drain current scales in proportion to the number of nanowires participating in charge transport.

Assuming ohmic contact between PbSe and Au, we can estimate the conductivity of the  $8$  nm diameter PbSe nanowires as  $\sim 10^2$  S  $\text{cm}^{-1}$ . This value is about 2 orders of magnitude higher than the electronic conductance of an array of quantum mechanically coupled  $8$  nm PbSe nanocrystals doped with hydrazine.<sup>25</sup> The high conductance originates primarily from the high carrier concentration in hydrazine treated PbSe nanowires.

Our estimates of a linear regime mobility for electrons in hydrazine-doped PbSe nanowire devices give values of  $9 \text{ cm}^2/\text{V s}$ . The mobility was calculated from the transconductance of a device with 18 parallel PbSe nanowires bridging the FET channel (Figure 4). The exact number of PbSe nanowires aligned between Au source and drain electrodes was obtained from SEM analysis of the device after the measurements. To calculate the capacitance of the gate dielectric layer, we used the Wunnicke approach based on a finite elements method,<sup>26</sup> which is more suitable for sub- $10$  nm nanowires than a cylinder on an infinite plate model typically used for larger (e.g.,  $40$  nm diameter) nanowires.<sup>27</sup> Taking into account that some nanowires might not be properly contacted or had structural defects, this mobility value should be considered as a conservative estimate. The current through the PbSe nanowire may be limited by the injection of carriers from Au electrodes into the nanowires. This could also explain why the electron mobility observed for PbSe nanowires is lower than the mobility in bulk PbSe ( $\sim 1500 \text{ cm}^2/\text{V s}$ ). Lowering the contact resistance between nanowires and electrodes is expected to improve the performance of the PbSe nanowire FETs.

The electrical properties of zigzag and branched PbSe nanowire FETs are similar to the properties of straight PbSe nanowire devices. As-synthesized all PbSe nanowires demonstrated a  $p$ -type gate effect that could be switched to an  $n$ -type by exposure to hydrazine solutions. However, nanowires with zigzag and branched morphologies have a larger spread in conductivity as compared to straight nanowires. This is consistent with the larger variations in diameter and with possible higher average concentrations of structural defects.<sup>15</sup> The nanoropes self-assembled from branched PbSe nanowires (Figure 3a,b) showed good electrical conductivity with nonlinear  $I$ – $V$  characteristics (Figure S2 in Supporting Information).

The possibility of doping the nanowires by exposing them to hydrazine or other charge-transfer dopants can be very useful for assembling nanowire circuits. Using electric fields for nanowire alignment has serious limitations in the case of highly conductive semiconductor nanowires because the large electric bias can cause a breakdown of the nanowires after they bridge the gap between source and drain electrodes. In the case of single-wire devices, this problem can be solved by switching off the electric bias immediately after the nanowire bridges the electrodes.<sup>20</sup> However, this technique cannot be applied to multiwire devices. To overcome this limitation, we first aligned poorly conducting undoped nanowires followed by the on-chip doping of the nanowires. We believe that this can be a powerful general approach for designing and fabricating nanowire circuits. Local exposure of nanowires to charge-transfer dopants like hydrazine (e.g., by inkjet printing) can provide local  $n$ -type doping while other parts of the circuit will remain insulated or  $p$ -doped.

**On-Chip Growth of PbSe Nanowires.** Rational design of nanowire electronic circuitry requires precise positioning of individual wires. Here, we demonstrate that an electric field can induce the formation of semiconducting nanowires from nanocrystal building blocks directly on a silicon chip. PbSe nanocrystals thoroughly washed to remove excess capping ligands slowly assemble into nanorods by oriented attachment of surfactant-depleted PbSe nanocrystals (Figure 5a). In a dc electric field, these nanorods, in turn, assemble into long wires that grow between biased Au electrodes (Figure 5b–d). The nanowire growth is caused by field-directed assembly of PbSe nanorods. Electric field concentrates at the end of the growing nanowire, attracting PbSe nanorods from the surrounding

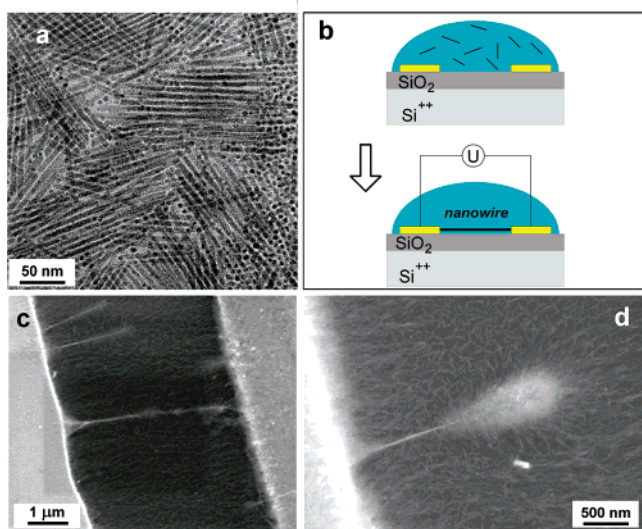


**Figure 5.** Electric field-directed on-chip assembly of PbSe nanowires. (a) PbSe nanorods used as soluble building blocks for nanowire assembly. (b) Schematics of the nanowire formation. (c and d) SEM images of growing PbSe nanowires.

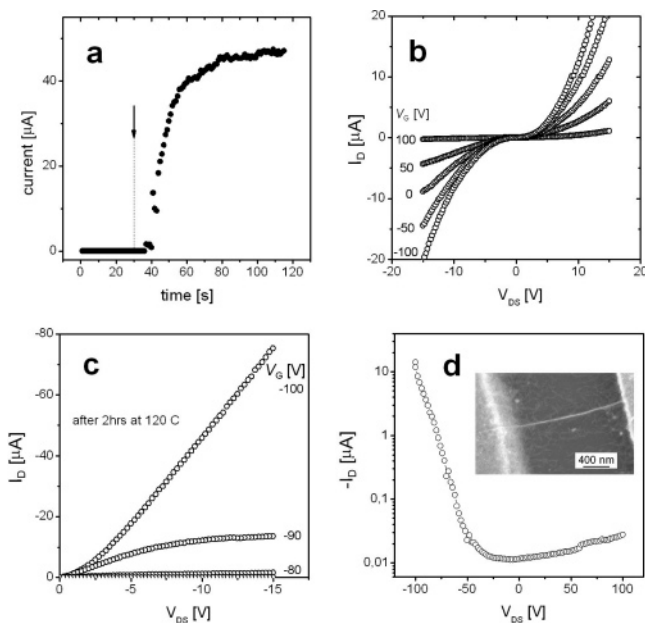


**Figure 6.** (a) Temporal evolution of the current between biased Au electrodes during nanowire growth. Arrow shows the instant of bias turn on. (b) Plot of drain current  $I_d$  vs drain-source voltage  $V_{ds}$ , as a function of gate voltage  $V_g$  for on-chip grown PbSe nanowires. (c) Plot of  $I_d$  vs  $V_{ds}$ , as a function of gate voltage  $V_g$  for the same PbSe nanowires after annealing at 120 °C for 2 h (d). Plot of  $I_d$  vs  $V_g$  measured at a constant  $V_{ds}$  of  $-4$  V for PbSe nanowires after annealing. Inset shows SEM image of on-chip grown PbSe nanowires annealed at 120 °C.

solution and extending the nanowires toward the opposite electrode. The “corona” from PbSe nanorods pulled toward the tip of the growing nanowire is shown in Figure 5d. This image was obtained by quenching the wire formation at an early stage and evaporating the solvent. Formation of PbSe nanowires is a collective effect, similar to dielectrophoretic assembly of gold nanoparticles in aqueous solutions.<sup>28</sup>

The assembled nanowires can conduct an electrical current (Figure 6a) and show a  $p$ -type gate effect (Figure 6b). As-grown nanowires can similarly be converted from  $p$ - to  $n$ -type by hydrazine treatment. The good electronic characteristics and mechanical stability of self-assembled PbSe nanowires suggests at least partial fusion of PbSe nanorods into single- or poly-

crystalline nanowires. Annealing chips with assembled nanowires on a hot plate at 120 °C for 120 min under nitrogen results in a substantial increase in FET on currents. Annealing also improves the conductance at low bias and the linearity of  $I$ – $V$  characteristics of our nanowire devices (Figure 6c). Field-effect transistors based on annealed on-chip grown PbSe nanowires show a  $p$ -type transport with current modulation on the order of  $10^3$  (Figure 6d). To the best of our knowledge, this is the first demonstration of electric field-guided assembly of semiconducting nanowires from pre-synthesized nanoscale building blocks into functional electronic devices. Both before and after annealing, PbSe nanowires demonstrated photocurrent generation shown in Figure S3 in the Supporting Information. The nanowires demonstrated a slow photoresponse indicative of long-lived trap states, presumably associated with the nanowire surface and grain boundaries.

## Conclusion

We demonstrated the techniques for assembling chemically synthesized semiconductor nanowires into functional field-effect devices and photodetectors. In addition to the low cost and high yield, colloidal synthesis allows for precise design of the nanowire morphology, providing novel ideas for nanowire devices. For example, conductive PbSe nanowires with a zigzag and branched morphology are promising for thermoelectric applications because their thermal conductivity is reduced by multiple scattering of acoustic phonons. PbSe nanowires might find use as photo- and electroluminescent materials emitting in the mid-IR spectral range. The on-chip assembly of high-mobility semiconducting nanowires may provide a novel concept for growing nanoscale electronic circuitry directly on a chip, in a way, similar to the formation of interconnects between neurons in biological systems. The approaches proposed in this work on the example of PbSe nanowires should be applicable to other  $II$ – $VI$ ,  $III$ – $V$ , and  $IV$ – $VI$  nanowires.

**Acknowledgment.** We thank Dr. Alex Henderson and Prof. Philip Kim (Columbia University) for electric measurements on single PbSe nanowires; Dr. C. H. Ben-Porat and Prof. Louis E. Brus (Columbia University) for EFM measurements; Dr. Brian Wehrenberg and Prof. Philippe Guyot-Sionnest (University of Chicago) for investigations of electrochemical doping of PbSe nanowires; and Robert L. Sandstrom (T. J. Watson Research Center, IBM) for technical support. Work at the Molecular Foundry was supported by the Director, Office of Science, Office of Basic Energy Sciences, Division of Materials Sciences and Engineering of the U.S. Department of Energy under Contract DE-AC02-05CH11231.

**Supporting Information Available:** TEM images of PbSe nanowires, transport characteristics of branched PbSe nanowires, and photocurrent generation by on-chip grown PbSe nanowires. This material is available free of charge via the Internet at <http://pubs.acs.org>.

## References and Notes

- (1) Cui, Y.; Zhong, Z.; Wang, D.; Wang, W. U.; Lieber, C. M. *Nano Lett.* **2003**, *3*, 149–152.
- (2) Huang, Y.; Duan, X.; Cui, Y.; Lathon, L. J.; Kim, K.-H.; Lieber, C. M. *Science* **2001**, *294*, 1313–1317.
- (3) Duan, X.; Huang, Y.; Lieber, C. M. *Nano Lett.* **2002**, *2*, 487–490.
- (4) Patolsky, F.; Zheng, G.; Hayden, O.; Lakadamyali, M.; Zhuang, X.; Lieber, C. M. *Proc. Natl. Acad. Sci. U.S.A.* **2004**, *101*, 14017–14022.
- (5) Lin, Y.-M.; Dresselhaus, M. S. *Phys. Rev. B* **2003**, *68*, 75304-1–75304-14.

- (6) Qian, F.; Gradecak, S.; Li, Y.; Wen, C.-Y.; Lieber, C. M. *Nano Lett.* **2005**, *5*, 2287–2291.
- (7) Duan, X.; Huang, Y.; Agarwal, R.; Lieber, C. M. *Nature* **2003**, *421*, 241–245.
- (8) Law, M.; Greene, L. E.; Johnson, J. C.; Saykally, R.; Yang, P. *Nat. Mater.* **2005**, *4*, 455–459.
- (9) Hayden, O.; Agarwal, R.; Lieber, C. M. *Nat. Mater.* **2006**, *5*, 352–356.
- (10) Gudiksen, M. S.; Wang, J.; Lieber, C. M. *J. Phys. Chem. B* **2001**, *105*, 4062–4064.
- (11) Law, M.; Goldberg, J.; Yang, P. *Annu. Rev. Mater. Res.* **2004**, *34*, 83–122.
- (12) Trentler, T. J.; Hickman, K. M.; Goel, S. C.; Viano, A. M.; Gibbons, P. C.; Buhro, W. M. *Science* **1995**, *270*, 1791–1794.
- (13) Penn, R. L.; Banfield, J. F. *Geochim. Cosmochim. Acta* **1999**, *63*, 1549–1557.
- (14) Tang, Z.; Kotov, N. A.; Giersig, M. *Science* **2002**, *297*, 237–240.
- (15) Cho, K.-S.; Talapin, D. V.; Gaschler, W.; Murray, C. B. *J. Am. Chem. Soc.* **2005**, *127*, 7140–7147.
- (16) Zhu, J.; Peng, H.; Chan, C. K.; Jarausch, K.; Zhang, X. F.; Cui, Y. *Nano Lett.* **2007**, *7*, 1095–1099.
- (17) Huang, Y.; Duan, X.; Wei, Q.; Lieber, C. M. *Science* **2001**, *291*, 630–633.
- (18) Jin, S.; Whang, D.; McAlpine, M. C.; Friedman, R. S.; Wu, Y.; Lieber, C. M. *Nano Lett.* **2004**, *4*, 915–919.
- (19) Harnack, O.; Pacholski, C.; Weller, H.; Yasuda, A.; Wessels, J. M. *Nano Lett.* **2003**, *3*, 1097–1101.
- (20) Duan, X.; Huang, Y.; Cui, Y.; Wang, J.; Lieber, C. M. *Nature* **2001**, *409*, 66–69.
- (21) Wang, D.; Zhu, R.; Zhou, Z.; Ye, X. *Appl. Phys. Lett.* **2007**, *90*, 103110.
- (22) Houtepen, A. J.; Koole, R.; Vanmaekelbergh, D.; Meeldijk, J.; Hickey, S. G. *J. Am. Chem. Soc.* **2006**, *128*, 6792–6793.
- (23) Fan, D. L.; Zhu, F. Q.; Cammarata, R. C.; Chien, C. L. *Appl. Phys. Lett.* **2004**, *85*, 4175–4177.
- (24) Shevchenko, E. V.; Talapin, D. V.; Kotov, N. A.; O'Brien, S.; Murray, C. B. *Nature* **2006**, *439*, 55–59.
- (25) Talapin, D. V.; Murray, C. B. *Science* **2005**, *310*, 86–89.
- (26) Wunnicke, O. *Appl. Phys. Lett.* **2006**, *89*, 83102.
- (27) Cui, Y.; Duan, X.; Hu, J.; Lieber, C. M. *J. Phys. Chem. B* **2000**, *104*, 5213–5216.
- (28) Hermanson, K. D.; Lumsdon, S. O.; Williams, J. P.; Kaler, E. W.; Velev, O. D. *Science* **2001**, *294*, 1082–1086.